# A study of fast reactor fuel transmutation in a candidate dispersion fuel design

**Mark D. DeHart, Hongbin Zhang, Eric Shaber**
Idaho National Laboratory
Idaho Falls, ID, United States

**Matthew A. Jessee**
Oak Ridge National Laboratory
Oak Ridge, TN, United States

## Abstract

*The Idaho National Laboratory is currently performing research in the development of an innovative dispersion fuel concept for a fast reactor design. This fuel has been specifically designed to meet the challenges of transuranic transmutation by providing an integral fission gas plenum within the fuel itself, to eliminate the swelling that accompanies the irradiation of TRU. This paper summarises the results of reactor physics calculations for a conceptual fuel design. The fuel consists of all transuranics (TRU) with plutonium and minor actinides representative of spent light water reactor (LWR) fuel after five years of cooling. A fuel and core design based on the conceptual Advanced Burner Test Reactor design is analysed to study the feasibility of a fast reactor based on the proposed fuel design. The results indicate that this fuel design could be used in a fast reactor spectrum for fuel transmutation, although current results do not show the level of actinide destruction seen in thermal reactor concepts. However, this very simple core design applied in these analyses has not been optimised, and improved performance may be possible with proper core design.*

## Introduction

Dispersion fuels represent a significant departure from typical ceramic fuels to address swelling and radiation damage in high burn-up fuel. Such fuels use a manufacturing process in which fuel particles are encapsulated within a non-fuel matrix. Dispersion fuels have been studied since 1997 as part of an international effort to develop and test very high density fuel types for the Reduced Enrichment for Research and Test Reactors (RERTR) programme [1]. Idaho National Laboratory is performing research in the development of an innovative dispersion fuel concept that will meet the challenges of transuranic (TRU) transmutation by providing an integral fission gas plenum within the fuel itself, to eliminate the swelling that accompanies the irradiation of TRU. In this process, a metal TRU vector produced in a separations process is atomised into solid microspheres. The dispersion fuel process overcoats the microspheres with a mixture of resin and hollow carbon microspheres to create a TRUC (transuranic carbide) fuel. The foam may then be heated and mixed with a metal powder (e.g. Zr, Ti or Si) and resin to form a matrix metal carbide, that may be compacted and extruded into fuel elements.

Reactor physics calculations have been performed for a conceptual fuel design to assess the feasibility of a dispersion fuel in a fast reactor design. The fuel was assumed to consist of transuranics (TRU) only, with plutonium and minor actinides representative of spent light water reactor (LWR) fuel after five years of cooling. A fuel and core design based on the Advanced Burner Test Reactor (ABTR) design [2] is employed. The CSAS6 and TRITON modules of the SCALE system [3] have been used for these preliminary scoping studies.

## Analysis

### *Fuel composition*

Because this is a scoping study, exact fuel specifications are not available, and some assumptions were made. For the fuel itself, estimates of likely composition and fabrication parameters were provided by INL materials staff. The assumed TRU composition is provided in Table 1. The anticipated fuel fabrication process will provide grains with a 1:1 metal to graphite ratio with 50% void content. A grain density of 6 g/cm$^3$ was assumed. An average particle radius of 100 μm was specified, which includes a 10 μm thick coating of ZrC, with a density of 6.73 g/cm$^3$. The grains are dispersed within natural zirconium.

**Table 1: TRU metal composition**

| Nuclide | Fraction (wt.%) |
|---|---|
| $^{237}$Np | 6.79 |
| $^{238}$Pu | 2.90 |
| $^{239}$Pu | 49.43 |
| $^{240}$Pu | 22.97 |
| $^{241}$Pu | 8.79 |
| $^{242}$Pu | 4.90 |
| $^{241}$Am | 2.80 |
| $^{242m}$Am | 0.02 |
| $^{243}$Am | 1.40 |

### *Pin cell calculations*

A pin cell model was developed based on the ABTR specification, as shown in Figure 1. The fuel column is surrounded by sodium as a thermal bound, with HT-9 clad and a HT-9 wire wrap. Sodium is also used as a coolant. The ABTR was designed with a 80 cm fuel stack below a 120 cm fission gas plenum. Because the proposed fuel is designed to retain fission products, no plenum


ACTINIDE AND FISSION PRODUCT PARTITIONING AND TRANSMUTATION, ISBN 978-92-64-99174-3, © OECD 2012

**Figure 1: ABTR pin cell dimensions [2]**

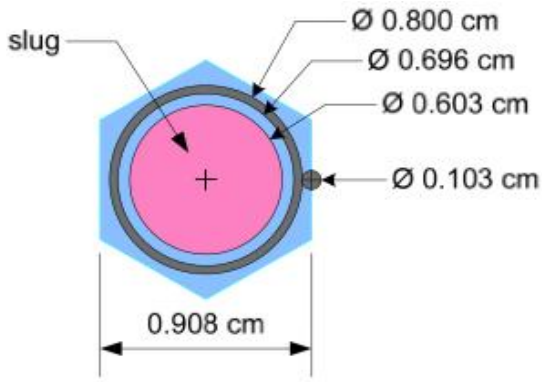


is needed, and a 200 cm axial fuel height was assumed. The fuel column was assumed to be at a constant temperature of 793 K, with the sodium bond at 780 K, and cladding, wire wrap and coolant at 750 K.

This fuel design is similar to that of current very high-temperature reactor (VHTR) designs in the sense that encapsulated fuel grains are randomly dispersed within a non-fuel matrix. In the thermal spectrum of a VHTR, the size of fuel grains is not negligible with respect to the neutron mean free path at resonance and thermal energies, and a doubly-heterogeneous fuel treatment is required for multi-group resonance processing [4]. Intuitively, one would expect that the mean free path of fast neutrons in a fast reactor design would be significantly larger than the grain size in the proposal dispersal fuel. However, because of the uniqueness of the proposed fuel design, it was felt to be appropriate to test this assertion before proceeding. Hence, two ABTR-type pin cell models were developed for the fuel cell: in the first, a SCALE double-heterogeneity treatment was applied for particles randomly distributed with a zirconium matrix with a 50% volume fraction; in the second model, materials were homogenised by volume weighting fuel grain, coating and zirconium number densities. Table 2 lists the compositions used in the two models. KENO-VI was used to perform the eigenvalue calculations using the CSAS6 sequence with CENTRM continuous-energy resonance self-shielding calculations and the SCALE ENDF/B-VII library to create a 238-group weighted library.

Results of these calculations are given in Table 3. Although the two $k_{inf}$ values are not statistically identical, the difference between the two approaches is less that 0.1%. Hence, all remaining calculations were performed using homogenised fuel models.

The above results also indicate that a pin cell model with a 50% volume fraction provides significant excess reactivity, which is necessary to offset the reactivity loss due to leakage, spectral changes, and absorption in non-fuel elements. However, because the volume fraction of coated TRUC particles within the fuel element was not specified, and a 50% volume fraction seems perhaps large from a material fabrication perspective (the maximum packing fraction for spherical bodies is 74%, and random close packing is limited to approximately 63%). Thus, additional pin cell calculations were performed in which the volume fraction was allowed to vary from 10 to 70% within an infinite lattice pin cell model to determine if a critical spectrum could be obtained.

Figure 2 illustrates the trend in $k_{inf}$ with increasing fuel packing – error bars are within the size of the symbols. Clearly, packing fractions of less than 10% will not yield a critical system – that still leaves a substantial margin for design calculations. Typically, LWR fuels have an infinite lattice multiplication factor on the order of 1.35, to account for reactor leakage and burn-up of other loaded fuel elements. For this design, fuel burn-up has not yet been considered, and a start-up core loaded with fresh fuel is assumed. However, significant leakage is anticipated due to the small size of the core. Hence, it is anticipated that a packing fractions in the range of 45-60% will be necessary for use in a fast reactor environment.

**Table 2: Fuel rod compositions for dispersed and homogenised models**

| Nuclide | Doubly-heterogeneous model | Homogenised model |
|---|---|---|
| **Zirconium matrix** *(50% volume)* | | |
| $^{90}$Zr | 2.2044E-02 | 1.1022E-02 |
| $^{91}$Zr | 4.8072E-03 | 2.4036E-03 |
| $^{92}$Zr | 7.3479E-03 | 3.6739E-03 |
| $^{94}$Zr | 7.4464E-03 | 3.7232E-03 |
| $^{96}$Zr | 1.1997E-03 | 5.9983E-04 |
| **ZrC grain coating** *(13.55% volume)* | | |
| C | 3.9435E-02 | 5.3434E-03 |
| $^{90}$Zr | 2.0289E-02 | 2.7492E-03 |
| $^{91}$Zr | 4.4246E-03 | 5.9953E-04 |
| $^{92}$Zr | 6.7631E-03 | 9.1640E-04 |
| $^{94}$Zr | 6.8538E-03 | 9.2869E-04 |
| $^{96}$Zr | 1.1042E-03 | 1.4962E-04 |
| **TRUC** *(36.45% volume)* | | |
| C | 2.1043E-02 | 7.6700E-03 |
| $^{237}$Np | 9.5253E-04 | 3.4720E-04 |
| $^{238}$Pu | 4.0682E-04 | 1.4829E-04 |
| $^{239}$Pu | 6.9342E-03 | 2.5275E-03 |
| $^{240}$Pu | 3.2223E-03 | 1.1745E-03 |
| $^{241}$Pu | 1.2331E-03 | 4.4946E-04 |
| $^{242}$Pu | 6.8739E-04 | 2.5055E-04 |
| $^{241}$Am | 3.9280E-04 | 1.4317E-04 |
| $^{242m}$Am | 2.8057E-06 | 1.0227E-06 |
| $^{243}$Am | 1.9640E-04 | 7.1587E-05 |

**Table 3: Comparison of explicit particle vs. homogenised treatments**

| TRUC (36.45% volume) | | |
|---|---|---|
| **Case** | **$k_{inf}$** | **Error ($\sigma$)** |
| Explicit DH fuel | 1.43466 | 0.00034 |
| Homogenised fuel | 1.43606 | 0.00033 |

**Figure 2: $k_{inf}$ as a function of fuel particle volume fraction for infinite lattice of pin cells**

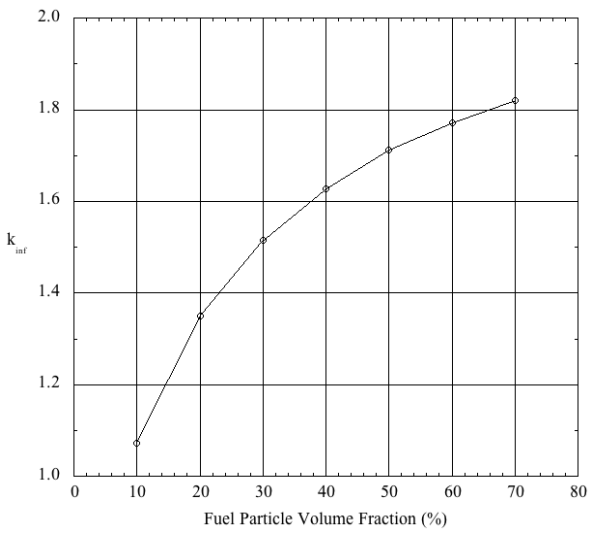

### *Reactor design*

As discussed earlier, the ABTR design was selected as a basis for a prototype design for the candidate fuel design in a fast-spectrum TRU burner, modified primarily by expanding the fuel height from 80 cm to 200 cm. A KENO-VI model of the ABTR core has been developed using 200 cm heights of TRU dispersion fuel, but otherwise closely followed the design of the ABTR core, as described in Ref. [2] and shown in Figure 3. For this work, the inner, outer and test positions were assumed to all be loaded with a single fuel enrichment – future work should consider inner/outer fuel enrichment splits as needed to flatten to core flux profile. Hence, the redesigned TRU-fuelled core consists of 63 fuel assemblies, 78 reflector assemblies, 48 shield assemblies, and 7 primary and 3 secondary control assemblies. Ref. [2] lacks detail on the axial design of some regions of the core, so engineering judgment was applied in finishing axial design where documentation was lacking. Figure 4 shows KENO-VI two-dimensional rendering of the core face.

**Figure 3: Core loading face map for ABTR design [2]**

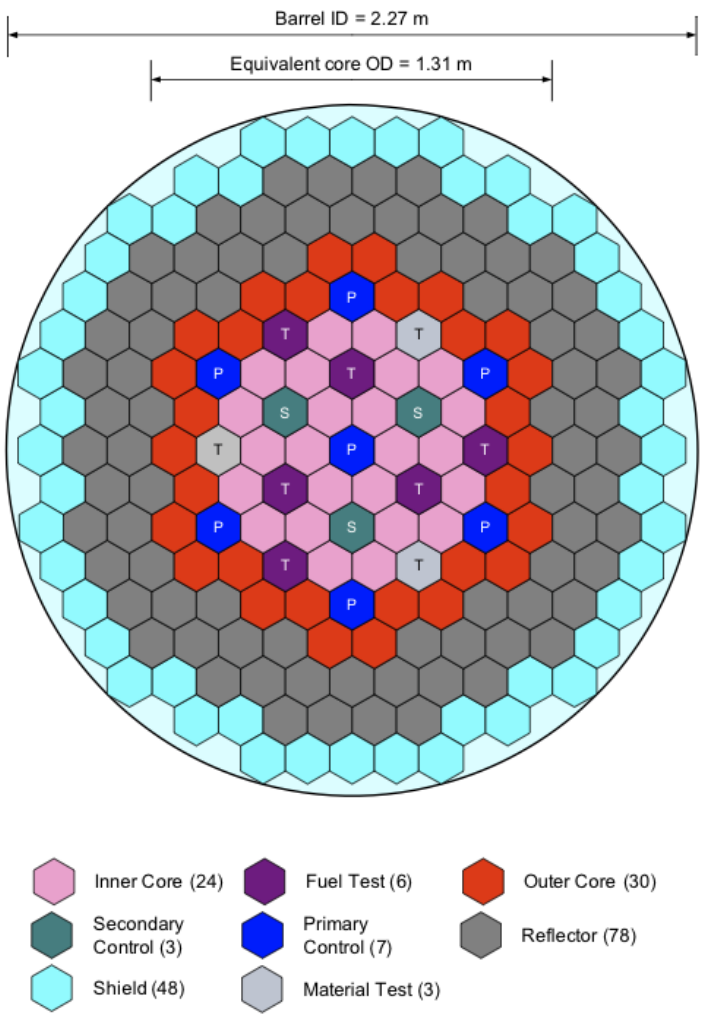

**Figure 4: KENO-VI core face map at axial mid-plane, with secondary control assemblies fully withdrawn**

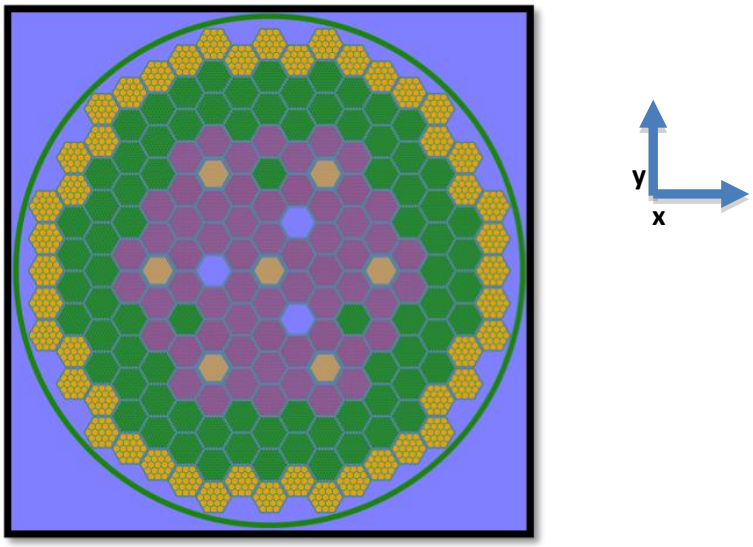


## Results

### *Design calculations*

In order to determine the appropriate volume fraction for the dispersed TRU design, a safe shutdown state was assumed. Typically for light water reactors, licensing requirements are such that the reactor must be shown to be subcritical when shut down, with $k_{eff}$ less than or equal to 0.99 with the core in its most reactive state (usually at room temperature), and with the most reactive control position completely withdrawn. For this work, a more conservative value of 0.98 was assumed to account for a number of un-quantified unknowns. Room temperature was assumed (although sodium is solid at this temperature), and the central control position was assumed to be fully withdrawn (filled with sodium). All remaining control assemblies were modelled as completely inserted. Volume fractions were varied from 30 to 60% fuel pellets in zirconium to find the fuel fraction that would yield a core $k_{eff}$ of 0.98 or less. Results of these calculations are shown in Figure 11 (error bars are smaller than the plot symbols). The desired fraction was determined to lie between 50 and 55%, and a tighter search was performed. Ultimately, a volume fraction of 53.4% in fuel particles was found to yield an acceptably low multiplication factor of 0.97956±0.00051 [note that from a purely regulatory point of view, this value would be too high, as 0.97956 is within one standard deviation (0.00051) of 0.98].

There are several other reactivities of interest for this fuel loading – additional calculations were performed for all control rods in under both cold and hot conditions, for secondary control assemblies withdrawn (hot) and for both secondary and primary control assemblies withdrawn (hot). Table 4 provides a summary of results for each calculation.

The ABTR is designed to operate with control assemblies present in the core; the control assemblies are withdrawn over the core lifetime to provide reactivity to maintain criticality with fuel burn-up. For this design, criticality can be achieved with the secondary control assemblies partially withdrawn. These control assemblies could be withdrawn independently or in tandem with the primary system. That is a design option beyond the scope of this study; for this work, it is assumed that secondary control is completely withdrawn before primary control assemblies start to be withdrawn. To understand the behaviour of the control systems, control assembly worth calculations were performed for first the secondary system then the primary system with secondary fully withdrawn. Figure 12 shows the increase in reactivity seen in the fresh core as first the secondary then the primary control systems are removed.

**Figure 11: $k_{eff}$ as a function of fuel particle volume fraction for full core design under limiting conditions**

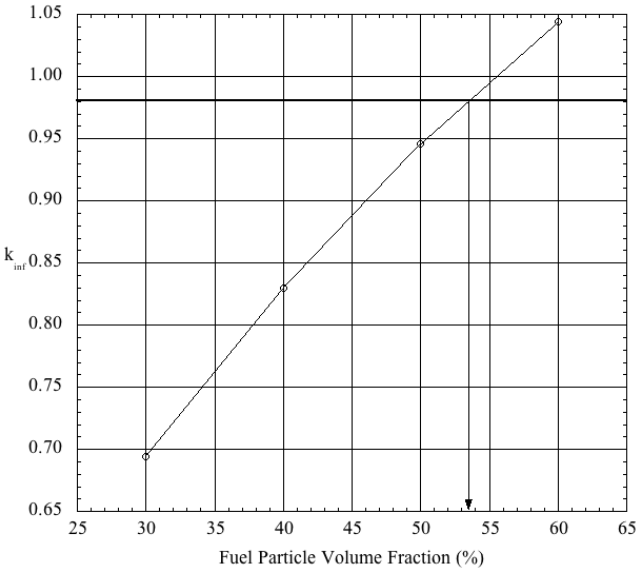


**Table 4: Reactivity properties of fresh core with dispersed TRU fuel**

| Case | State | $k_{eff}$ | Uncertainty (±σ) | Reactivity ρ (k-1/k) |
|---|---|---|---|---|
| Limiting (most reactive control assembly withdrawn) | Cold | 0.97742 | 0.00062 | -0.0115 |
| All rods in | Cold | 0.94191 | 0.00057 | -0.0617 |
| All rods in | Hot | 0.94096 | 0.00069 | -0.0627 |
| All secondary system control assemblies withdrawn | Hot | 1.03229 | 0.00069 | 0.0313 |
| All control assemblies withdrawn | Hot | 1.18844 | 0.00073 | 0.1586 |

**Figure 12: Fresh core $k_{eff}$ as a function of percentage of control system withdrawn**

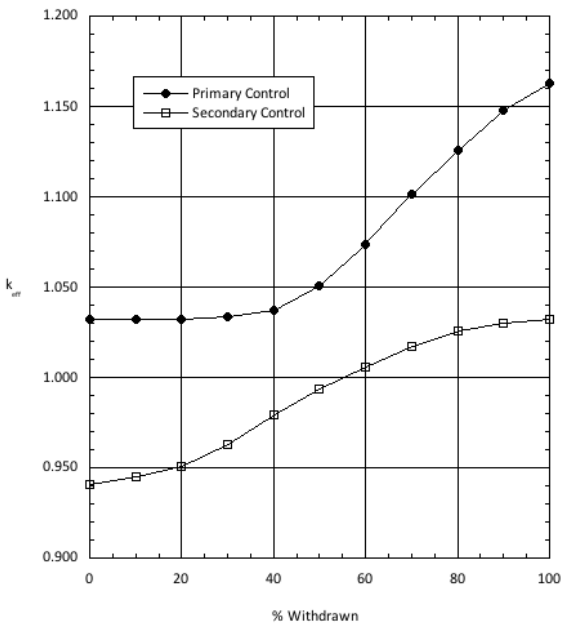

For BOL conditions, a criticality search determined that the core would be critical with the secondary control assemblies withdrawn 56% from full insertion.

### *Core depletion calculations*

Two key factors of interest in core design are the length of the burn-up cycle, and the isotopes present at discharge. The longer the reactor can operate, the more of the initial transuranics are consumed; the inventory at EOL, with an appropriate cooling time, will indicate the net transuranic depletion. At this point a scoping estimate is desired, so a detailed core design is not attempted. Hence, no refuelling or core shuffling was attempted. Calculations were performed assuming uniform burn-up across the core (i.e. the core was modelled with a single depletion material using the average flux within that material). All materials within core containing boron were depleted. Control rods were assumed to be withdrawn with burn-up so as to maintain criticality; secondary rods were withdrawn first, followed by primary rods. End of life was defined as the time at which all primary rods were fully withdrawn. A five-year cooling time was assumed post-discharge for isotopic inventory calculations. Depletion calculations were performed using the TRITON T6-DEPL sequence of SCALE, which couples KENO-VI with ORIGEN for depletion calculations. A power density of 170 MW/tonne heavy metal was determined based on the nominal core power. Fast-running (small number of neutron histories) KENO-VI calculations were used to estimate control rod positions such that $k_{eff}$ remained within the range of 1.0±0.005 for each depletion calculation to maintain a critical spectrum throughout the burn-up cycle. The calculation was then rerun with a sufficient number of neutron histories to be able to accurately capture the spectrum in each depletion material.

Given this simplistic approach to core design, the core was able to maintain criticality for approximately 950 days, at which time all control rods were withdrawn. Figure 13 illustrates the behaviour of $k_{eff}$ as a function time, and also shows the total burn-up density.

**Figure 13: Average fuel burn-up and $k_{eff}$ approximation used as a function of time**

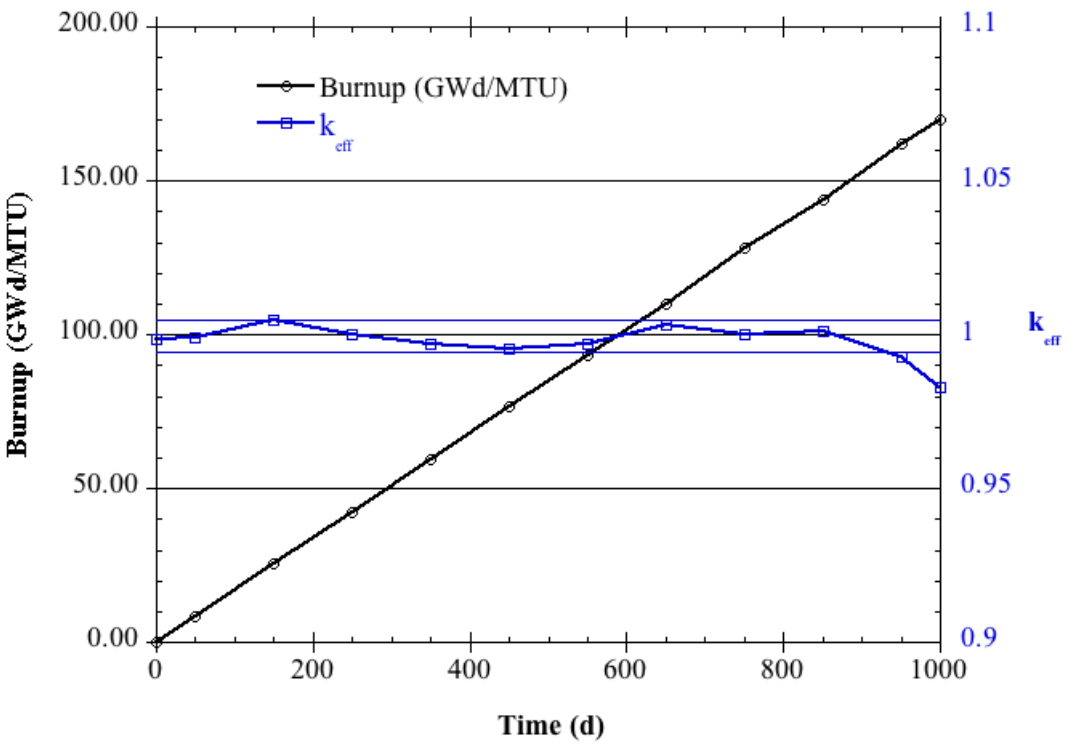

Table 5 presents the results of depletion calculations for end of cycle (after 950 d in core) and after an additional 5 y cooling time. A net total of 17.8% of the higher actinide inventory has been completely destroyed, comprised primarily of $^{237}$Np, $^{239}$Pu and $^{241}$Pu. The destruction is offset by net production of $^{238}$Pu, $^{240}$Pu, $^{241}$Am, $^{242m}$Am and $^{243}$Am, along with the creation of a number of curium isotopes and small amounts of uranium. The remaining actinides omitted from the table amount to approximately 0.0066% of the total mass at discharge and 0.00025% after five years. Figures 14 and 15 illustrate the relative distribution of isotopes at beginning of life and five years after discharge; the missing "piece of pie" in Figure 15 represents the mass of TRU destroyed. The figures make it clear that the TRU destruction is primarily $^{239}$Pu, $^{241}$Pu and $^{237}$Np. A number of the additional actinides shown in Figure 15 are produced from capture and capture/decay sequences, but their combined mass is quite small.

**Table 5: Results of depletion calculations for fast TRU-based system**

| Nuclide | Fuel actinide inventory (kg)* | | | | |
|---|---|---|---|---|---|
| | Charge | 950 d burn | 5 y cooled | % change | Absolute change (kg) |
| $^{234}$U | 0 | 0.658 | 2.158 | – | 2.158 |
| $^{235}$U | 0 | 0.054 | 0.102 | – | 0.102 |
| $^{236}$U | 0 | 0.066 | 0.187 | – | 0.187 |
| $^{237}$Np | 67.2 | 48.3 | 48.6 | -30.1% | -18.57 |
| $^{238}$Pu | 28.8 | 38.0 | 38.0 | 29.5% | 9.23 |
| $^{239}$Pu | 493.0 | 341.0 | 341.0 | -34.0% | -152.1 |
| $^{240}$Pu | 230.0 | 233.0 | 233.0 | 1.3% | 3.1 |
| $^{241}$Pu | 88.4 | 62.5 | 49.1 | -49.5% | -39.34 |
| $^{242}$Pu | 49.5 | 50.4 | 50.4 | 1.8% | 0.88 |
| $^{241}$Am | 28.2 | 27.8 | 40.9 | 44.2% | 12.75 |
| $^{242m}$Am | 0.2 | 1.19 | 1.16 | 187.4% | 0.957 |
| $^{243}$Am | 14.2 | 13.9 | 13.9 | -2.1% | -0.3 |
| $^{242}$Cm | 0 | 1.55 | 0.004 | – | 0.004 |
| $^{243}$Cm | 0 | 0.059 | 0.052 | – | 0.052 |
| $^{244}$Cm | 0 | 3.14 | 2.59 | – | 2.59 |
| $^{245}$Cm | 0 | 0.175 | 0.175 | – | 0.175 |
| $^{246}$Cm | 0 | 0.005 | 0.005 | – | 0.005 |
| *Destroyed* | *0* | *178.0* | *178.0* | | |

* Actinides with masses < 1g have been omitted.

**Figure 14: Illustration of isotopic composition of initial TRU fuel**

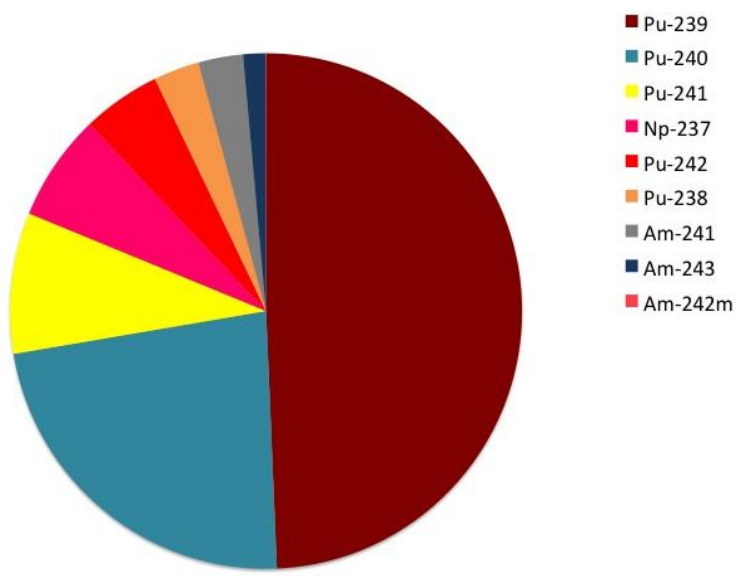

**Figure 15: Illustration of isotopic composition of irradiated fuel 5 y after discharge**

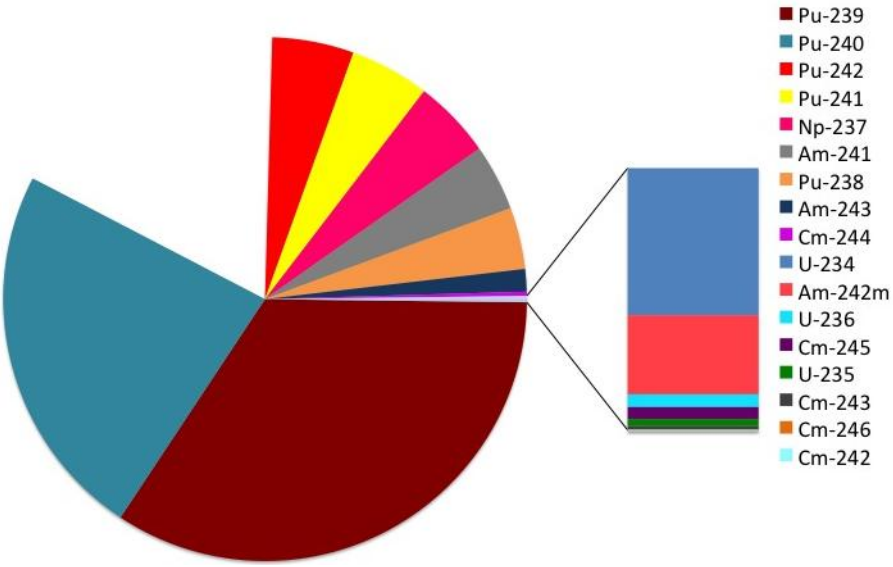


These results are consistent with calculations performed for TRU deep burn in a block-type modular gas reactor design [5]. The referenced work used a detailed core management analysis to optimise burn-up and obtained substantially more actinide destruction (61.5%). The TRU content used in their analysis is very similar to that used here, but has a different distribution of discharge products. Because the thermal gas reactor system has undergone detailed core design analysis to optimise TRU destruction, it is difficult to compare the performance of the two systems. However, it may be instructive to compare the relative production and loss of various nuclides in the fuel, because of the spectral differences between the two designs. To be able to make such a comparison, results obtained for the two designs are normalised to a per-kg-destroyed basis. Table 6 lists the masses destroyed in each design, and the fraction of the total destruction

**Table 6: Relative destruction and production of actinides in fast and thermal spectra**

| Nuclide | Proposed fast design | | Gas-cooled deep burn design | |
|---|---|---|---|---|
| | Kg destroyed | Kg destroyed per total mass destroyed | Kg destroyed (calculated from Ref. [5]) | Kg destroyed per total mass destroyed |
| $^{234}$U | 2.16 | -1.2% | 0.4 | -0.2% |
| $^{235}$U | 0.10 | -0.06% | 0.05 | -0.03% |
| $^{236}$U | 0.19 | -0.1% | 0.02 | -0.01% |
| $^{237}$Np | -18.6 | 10.4% | -12.7 | 6.81% |
| $^{238}$Pu | 9.2 | -5.2% | 9.8 | -5.3% |
| $^{239}$Pu | -152.1 | 85.4% | -147.2 | 78.9% |
| $^{240}$Pu | 3.1 | -1.7% | -52.7 | 28.3% |
| $^{241}$Pu | -39.3 | 22.1% | -11.1 | 5.9% |
| $^{242}$Pu | 0.9 | -0.5% | 19.3 | -10.4% |
| $^{241}$Am | 12.8 | -7.2% | -6.9 | 3.7% |
| $^{242m}$Am | 0.96 | -0.5% | 0.01 | -0.01% |
| $^{243}$Am | -0.3 | 0.2% | 6.2 | -3.3% |
| $^{242}$Cm | 0.004 | -0.0% | 0.7 | -0.4% |
| $^{243}$Cm | 0.05 | -0.03% | 0.04 | -0.02% |
| $^{244}$Cm | 2.6 | -1.5% | 7.1 | -3.8% |
| $^{245}$Cm | 0.18 | -0.1% | 0.4 | -0.2% |
| $^{246}$Cm | 0.005 | -0.0% | 0.1 | -0.05% |
| *Total* | *-178.0* | *-100%* | *-186.4* | *-100.0%* |


ACTINIDE AND FISSION PRODUCT PARTITIONING AND TRANSMUTATION, ISBN 978-92-64-99174-3, © OECD 2012

associated with each nuclide. Negative percentages indicate a net production of a given nuclide. Clearly, both systems are effective in the destruction of $^{239}$Pu; this is hardly surprising, as this represents the primary fissile nuclide present at beginning of life. $^{238}$Pu is also destroyed at about the same rate in both systems, while $^{237}$Np is destroyed at twice the rate in the fast system relative to the thermal system. The thermal deep burn system is more effective at $^{240}$Pu destruction, while $^{241}$Pu is destroyed more effectively in the conceptual fast system, while the fast system produces substantially more $^{242m}$Am than the thermal system. The fast system is a net producer of $^{241m}$Am, while the thermal system produces a net destruction of this nuclide.

### *Alternate fuel design*

The calculations described to this point are based on the ABTR fuel design illustrated in Figure 1. Because the current fuel design concept is not anticipated to release fission gasses, the gas plenum of the ABTR fuel design was replaced with fuel. However, in the scoping studies described above, the sodium gap was retained in the TRU fuel assembly design. Because of the nature of this design, little swelling would be anticipated, and it should be possible to co-extrude the fuel matrix to the cladding without the sodium bond. This would increase the volume available within each rod for the fuel matrix, and allow a reduced packing fraction for the fuel particles. The calculations described earlier and illustrated in Figure 11 for the core design were repeated assuming the sodium bond shown in Figure 1 was removed and replaced with the fuel matrix material. Figure 16 shows the plot of $k_{eff}$ versus fuel grain packing fraction for the modified fuel design. Clearly, the packing fraction can be reduced substantially, to a value on the order of 36-37%, to obtain a safely subcritical state under limiting conditions. This packing fraction would be much easier to attain in a practical manufacturing process.

**Figure 16: $k_{inf}$ as a function of fuel particle volume fraction for fuel design with no sodium bonding**

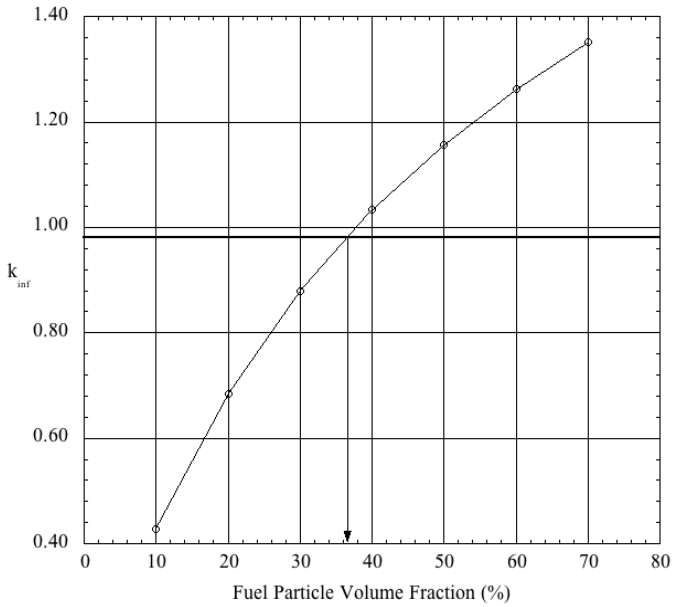


## Conclusions

Ongoing research at the INL involves the development of a new dispersion fuel concept that will meet the challenges of TRU transmutation by providing an integral fission gas plenum within the fuel itself. It is expected that this design will eliminate the swelling that typically accompanies the irradiation of TRU. However, the ability to fabricate such a fuel is of limited value unless the fuel can be demonstrated to be feasible for a reactor system.

In this work, a fast reactor design is developed based on the ABTR design concept proposed by Argonne National Laboratory to study the reactor physics performance of the proposed fuel design. Scoping analysis shows that this fuel design could indeed operate a fast reactor system. A fuel grain packing fraction ranging from 36-54% by volume within a zirconium matrix would provide sufficient reactivity to operate continuously for 2.5-3 years without any type of refuelling. The actual packing fraction required would depend on the use and thickness of a sodium bond between fuel and cladding.

The calculations performed in this report show that for a very simple fuel cycle, this approach would destroy about 18% of the TRU in the fuel. This is significantly less than that that has been reported in calculations for other designs; hence a more optimised fuel cycle design would likely be necessary to improve TRU destruction. Certainly and increased packing fraction to increase fuel reactivity combined with an appropriate burnable absorber would increase the core lifetime and TRU destruction. Alternatively, multi-cycle operation with fuel shuffling may be prescribed. Nevertheless, this work shows that a fast reactor fuelled with this advanced fuel type is feasible, and that further design studies are warranted.

## References

[1] Lemoine, P., D. Wachs, "High Density Fuel Development for Research Reactors", *Proc. of GLOBAL 2007 – Advanced Nuclear Fuel Cycles and Systems*, Boise, ID, United States, 9-13 September (2007).

[2] Chang, Y.I., *et al.*, *Advanced Burner Test Reactor Preconceptual Design Report*, ANL-ABR-1 (ANL-AFCI-173), Argonne National Laboratory, 5 September (2006).

[3] *SCALE: A Modular Code System for Performing Standardized Computer Analyses for Licensing Evaluations*, ORNL/TM-2005/39, Version 6.0, Vols. I-III, January (2009).

[4] DeHart, M.D., S. Goluoglu, J. Leppänen, "A Comparison of Deterministic and Monte Carlo Depletion Methods for HTGR Fuel Elements", *ANS Transactions*, 101 (2009).

[5] Kim, Y.H., F. Venneri, "Optimization of One-pass Transuranic Deep Burn in a Modular Helium Reactor", *Nucl. Sci. and Eng.*, 160, 59-74 (2008).